UNCLASSIFIED
CONFIDENTIAL

Copy 5
RM E56E04

NACA RM E56E04

NACA

RESEARCH MEMORANDUM

INVESTIGATION OF TURBINES SUITABLE FOR USE IN A TURBOJET ENGINE WITH HIGH COMPRESSOR PRESSURE RATIO AND LOW COMPRESSOR-TIP SPEED

VI - EXPERIMENTAL PERFORMANCE OF TWO-STAGE TURBINE

By Elmer H. Davison, Harold J. Schum, and Donald A. Petrash

Lewis Flight Propulsion Laboratory
Cleveland, Ohio

CLASSIFICATION CHANGED

To UNCLASSIFIED

By authority of TPA # 33 Date 10-28-60
ERG

CLASSIFIED DOCUMENT

This material contains information affecting the National Defense of the United States within the meaning of the espionage laws, Title 18, U.S.C., Secs. 793 and 794, the transmission or revelation of which is in any manner to an unauthorized person is prohibited by law.

NATIONAL ADVISORY COMMITTEE
FOR AERONAUTICS
WASHINGTON
August 20, 1956

LIBRARY COPY
AUG 23 1956
LANGLEY AERONAUTICAL LABORATORY
LIBRARY NACA
LANGLEY FIELD, VIRGINIA

CONFIDENTIAL
UNCLASSIFIED

[redacted] UNCLASSIFIED

NATIONAL ADVISORY COMMITTEE FOR AERONAUTICS

NASA Technical Library
3 1176 01435 8510

RESEARCH MEMORANDUM

INVESTIGATION OF TURBINES SUITABLE FOR USE IN A TURBOJET ENGINE WITH HIGH COMPRESSOR PRESSURE RATIO AND LOW COMPRESSOR-TIP SPEED

VI - EXPERIMENTAL PERFORMANCE OF TWO-STAGE TURBINE

By Elmer H. Davison, Harold J. Schum, and Donald A. Petrash

5016

CM-1

SUMMARY

As part of a general study of obtaining high work output at low blade speeds with multistage turbines, a two-stage turbine was experimentally investigated. High Mach numbers, high turning angles, and low static-pressure drops across blade rows made this a critical turbine design.

The turbine passed 1.01 of the equivalent design weight flow at equivalent design speed and work. The brake internal efficiency at this point was 0.79 and occurred at a rating pressure ratio of 4.1. A maximum efficiency of 0.84 occurred at 130 percent of equivalent design speed and a work output of 34.10 Btu per pound, corresponding to a rating pressure ratio of approximately 4.0.

A radial survey at equivalent design speed and work showed that the first-rotor throat area was too large; a large area of underturned flow also occurred near the tip of the rotor. A similar but less severe underturning was noted near the tip of the second rotor. Considerable underturning over most of the blade height at the outlet of the second stator was also observed. Tangential components of velocity at the turbine outlet amounting to 2.5 points in turbine efficiency were also measured.

INTRODUCTION

The NACA Lewis laboratory is currently conducting a general study of high-work-output, low-blade-speed, multistage turbines. As part of this study, the design requirements of turbines to drive a particular single-spool compressor with high pressure ratio and low blade tip speed were investigated at several engine operating conditions (ref. 1). It was found that operation at constant design rotative speed required a larger design turbine-outlet annular area than operation with constant exhaust-nozzle area. Further studies were made to determine the turbine velocity

[redacted] UNCLASSIFIED

diagrams for the turbine requirements imposed by engine operation with constant exhaust-nozzle area (ref. 2) and engine operation at constant design rotative speed (ref. 3). Based on the analyses presented in references 1 to 3, a turbine-outlet annular area of 405 square inches was specified for engine operations with constant exhaust-nozzle area and 550 square inches for engine operation at constant design rotative speed.

Because the turbine design requirements for engine operation at constant design rotative speed were more critical than those for engine operation with constant exhaust-nozzle area, it was necessary to incorporate a downstream stator behind a two-stage turbine in order to obtain reasonable velocity diagrams. These velocity diagrams and those for the two-stage turbine of reference 2 had higher Mach numbers, greater turning within blade rows, and lower static-pressure drops across some of the blade rows than those used in conventional turbine designs. Less critical turbine aerodynamic designs could, of course, have been obtained with three-stage turbines or by increasing the design rotative speed, as discussed in reference 4.

Although the two-stage turbine design for engine operation with constant exhaust-nozzle area and the two-stage turbine design with a downstream stator for engine operation at constant design rotative speed were critical, achievement of reasonably good turbine performance appeared to be feasible. However, only an experimental demonstration can verify this; therefore, a two-stage turbine and a two-stage turbine with a downstream stator were fabricated and investigated as components with cold-air turbine-inlet conditions. The performance of the two-stage turbine with a downstream stator is presented in reference 5. At equivalent design work and speed the brake internal efficiency of this turbine was 0.81, and the maximum efficiency obtained was 0.85. The downstream stator left very little energy in the form of tangential velocity in the gas and, in general, performed well with 0.78 recovery being obtained at equivalent design work and speed. The poor over-all performance of this turbine was attributed in part to the blade design procedure used, which appeared to be inadequate for a turbine with such critical aerodynamic limits. In addition, secondary-flow and tip-clearance effects that could not be accounted for in design may have contributed to the poor performance. The purpose of the subject report is to present and discuss the performance of the two-stage turbine.

The two-stage turbine was operated at a constant inlet total (stagnation) pressure of 35 inches of mercury absolute and an inlet total temperature of 700° R. Over-all turbine performance characteristics were obtained over a range of pressure ratios and speeds. These performance results are presented in terms of brake internal efficiency, equivalent work output, equivalent weight flow, and equivalent rotor speed.

In addition to the over-all performance, radial surveys of total pressure and flow angle were made behind each blade row and ahead of the

first stator at equivalent design work and speed. Radial distributions of temperature were obtained only behind the first and second rotors. Static-pressure distributions through the turbine were also obtained from interstage static-pressure measurements. The survey results are compared with the design distributions.

A brief description of the method used to design the blade profiles is also included.

3016

CM-1 back

SYMBOLS

A	annular area, sq ft
c_p	specific heat at constant pressure, Btu/(lb)(°R)
E	enthalpy drop (based on measured torque), Btu/lb
g	gravitational constant, 32.17 ft/sec^2
J	mechanical equivalent of heat, 778 ft-lb/Btu
N	rotational speed, rpm
p	static pressure, lb/sq ft
p'	total pressure, lb/sq ft
p'_x	rating total pressure, static pressure plus velocity pressure corresponding to axial component of velocity, lb/sq ft
R	gas constant, 53.35 ft-lb/(lb)(°R)
T	static temperature, °R
T'	total temperature, °R
V	velocity, ft/sec
w	weight flow, lb/sec
$\frac{wN}{60\delta}\varepsilon$	weight-flow parameter based on equivalent weight flow and equivalent rotor speed
α	absolute air angle, measured from axial direction (positive in direction of blade rotation), deg
γ	ratio of specific heats

δ ratio of inlet total pressure to NACA standard sea-level pressure of 2116 lb/sq ft

ε function of γ, $\dfrac{\gamma_{sl}}{\gamma_e} \dfrac{\left(\dfrac{\gamma_e + 1}{2}\right)^{\frac{\gamma_e}{\gamma_e - 1}}}{\left(\dfrac{\gamma_{sl} + 1}{2}\right)^{\frac{\gamma_{sl}}{\gamma_{sl} - 1}}}$

η brake internal efficiency, ratio of actual turbine work based on torque measurements to ideal turbine work

η_T internal efficiency based on measured total temperature

θ_{cr} squared ratio of critical velocity to critical velocity at NACA standard sea-level temperature of 518.7° R

ρ static density, lb/cu ft

τ torque, ft-lb

Subscripts:

e engine operating conditions

sl NACA standard sea-level conditions

0,1,2,3,4,5 measuring stations (see fig. 2)

APPARATUS

Test Installation

The experimental setup of the turbine is shown in figure 1. The air weight flow through the turbine was measured by a submerged calibrated A.S.M.E. flange-tap flat-plate orifice. After metering, the air was throttled to the desired turbine-inlet pressure of 35 inches of mercury absolute. A portion of this air was heated by two commercial jet-engine burners and reintroduced into the main airstream. The resulting turbine-inlet temperature after mixing was maintained at 700° R. The fuel flow was measured with rotameters in the fuel line, and the air weight flow through the turbine was corrected for the fuel addition. The air flow

divided and entered a plenum chamber (which replaced the normal combustor assembly of an engine) through two openings 180° apart and at right angles to the turbine shaft. The air then passed through a screen and into 10 transition sections, each of which supplied air to a segment of the first-stage stator. The air passed through the turbine into the tailcone, whence it was discharged into the laboratory exhaust facilities.

Two 5000-horsepower cradled dynamometers of the eddy-current wet-gap type were connected in tandem and were used to absorb the power output of the turbine. The turbine torque output was measured by means of an NACA balanced-diaphragm thrustmeter. The turbine rotative speed was measured by means of an electric chronometric tachometer.

5016

Instrumentation

The instrumentation used for the over-all performance evaluation of the turbine was located at stations 0, 1, and 5, as shown in figure 2. The conditions at the inlet of the transition section (station 0) were measured by means of a combination probe consisting of a shielded total-pressure tube and a calibrated spike-type thermocouple, and two wall static-pressure taps in each of the 10 transition sections. At station 1, static-pressure measurements were obtained from 20 static taps, one located on the inner and one on the outer wall of each of the 10 transition pieces. The instrumentation installed at station 5 consisted of five shielded total-pressure probes located at different radii corresponding to the area centers of five equal annular areas and of four wall static-pressure taps on both the inner and outer shrouds. Four thermocouple rakes were also installed at station 5. Each thermocouple rake consisted of five spike-type thermocouples located so that duplicate temperatures at 10 radial positions at the area centers of equal annular areas were obtained with the four rakes.

Additional fixed instrumentation was installed behind the first rotor blade row (station 3) consisting of two total-temperature rakes and five shielded total-pressure probes. The two total-temperature rakes each consisted of five thermocouples located so that the temperatures at 10 radial positions at the centers of equal annular areas were obtained. The five shielded total-pressure probes were located at different radii corresponding to the centers of five equal annular areas. Four static-pressure taps on both the inner and outer shrouds were also installed at stations 2, 3, and 4. These static-pressure taps were located approximately midway circumferentially between adjacent stator blades.

In addition to the fixed instrumentation, radial surveys of total pressure and angle were made at stations 1 to 5 with claw-type total-pressure probes. Photographs of the instrumentation used to obtain both general performance and survey data are shown in figure 3.

TURBINE AND BLADE DESIGN

Velocity Diagrams

The design velocity diagrams and the method used to select them are presented in reference 2. In calculating the design velocity diagrams at stations 2 to 5, a free-vortex distribution of tangential velocity and simple radial equilibrium were assumed. Radial components of velocity were ignored in calculating the velocity diagrams as well as in the design of the blade profiles. These design velocity diagrams are reproduced from reference 2 and presented in figure 4.

Turbine Blade Profile Design

The blade profiles were designed using a two-dimensional quasi-channel-flow theory and a stream-filament technique developed in reference 6.

Three flow regions were examined for each constant-radius blade-passage design. These three regions consisted of (1) the section between the passage potential line where the flow first becomes fully contained within the blade passage and the passage potential line at the throat of the blades, (2) the portion of the blade downstream of the throat, and (3) the leading-edge section of the blade. The design procedure consisted of mating these three flow regions by means of judicious selection of blade profiles until a reasonable compromise of the flow conditions was achieved. The passage throat and blade portion downstream of it were assumed to control the exit flow angle. For the leading-edge sections, high-speed NACA 65-series airfoil nose sections were used. In the channel portion of the blade the surface velocities were calculated by use of the stream-filament technique of reference 6; the maximum suction-surface Mach number and the maximum ratio of suction-surface velocity to exit velocity encountered were quite high, being 1.45 and 1.60, respectively.

The design blade profiles obtained in this manner are shown in figure 5.

Blade Solidity and Aspect Ratio

In order to save time in fabricating the turbine, existing turbine rotor disks and shell structure from a commercial turbine were used, which precluded the free choice of blade solidities and aspect ratio. The resulting solidities and aspect ratios based on axial chord were as follows:

	Solidity			Mean aspect ratio
	Hub	Mean	Tip	
Stator 1	1.361	1.240	1.140	1.78
Rotor 1	1.473	1.321	1.218	2.09
Stator 2	1.879	1.666	1.498	2.08
Rotor 2	1.978	1.608	1.334	2.09

5016

Turbine

The two-stage turbine was designed for the following conditions:

	Turbine design conditions	Turbine equivalent design conditions
Work, Btu/lb	131	32.25
Weight flow, lb/sec	158	39.65
Rotative speed, rpm	6100	3027
Inlet temperature, $^{\circ}R$	2160	518.7
Inlet pressure, in. Hg abs	248.3	29.92

A schematic diagram of the geometry employed in the turbine design is shown in figure 2. In the design the turbine frontal area was required to be no larger than the compressor frontal area. Because of this restriction on turbine frontal area and the low design rotative speed, the velocity diagrams were obtained by keeping the tip diameter of the turbine constant and obtaining all the area divergence through the turbine from the inner wall. The tip diameter of the turbine was constant at 33.5 inches; the annular area increased through the turbine, the inner shroud having a cone half-angle of 13.9°. The hub-tip radius ratios at the outlets of the first stator and last rotor were, respectively, 0.827 and 0.736. The turbine was designed to produce 70 percent of the design work output in the first stage and 30 percent in the second stage.

METHODS AND PROCEDURES

The turbine was operated with a measured inlet pressure p_0' of approximately 35 inches of mercury absolute and an inlet temperature T_0' of 700° R for equivalent rotative speeds of 20, 40, 60, 70, 80, 90, 100, 110, 120, and 130 percent of the design value. A range of rating pressure ratios $p_1'/p_{x,5}'$ from 1.4 to 4.1 was investigated.

The method used to convert turbine test conditions to equivalent operating conditions based on NACA standard sea-level conditions is given in reference 7. The equivalent work output and brake internal efficiency for the over-all performance are based on measured torque values.

The over-all turbine performance rating was based on the calculated outlet pressure $p'_{x,5}$ and calculated inlet pressure p'_1. The calculated outlet pressure $p'_{x,5}$ is defined as the static pressure behind the last rotor plus the velocity pressure corresponding to the axial component of the absolute velocity. This calculated value of turbine-outlet pressure charges the turbine for the energy of the tangential component of outlet velocity. This pressure is calculated from the energy and continuity equations by using the known annulus area at the measuring station and measured values of weight flow, static pressure, total (stagnation) pressure, and total temperature. The derivation of the equation to calculate $p'_{x,5}$ is given in the appendix of reference 5. The derivation of the equation to calculate p'_1 is given in the appendix herein. In calculating the inlet total pressure p'_1 from equation (5) of the appendix it was assumed that the flow was axial. The total temperature measured at station 0, the measured weight flow, the static pressure at station 1, and the annulus area at station 1 were used to calculate p'_1.

5016

The total temperatures at stations 0 and 5 and the total pressures at station 5 were arithmetically averaged for a single reading of temperature and pressure at each of these stations. In presenting the static-pressure distribution through the turbine, the arithmetic average of the hub wall static-pressure readings was used for stations 1 to 5. In calculating $p'_{x,5}$ and p'_1, the wall static-pressure readings at both the hub and tip were arithmetically averaged for a single reading.

The indicated temperature readings obtained from the spike-type thermocouple probes were corrected for Mach number effects. The indicated pressure readings obtained from the shielded total-pressure probes and claw-type total-pressure probes were also corrected for Mach number effects.

In addition to the general performance, radial total-pressure and angle surveys were made with the claw probe shown in figure 3(b) at stations 1 to 5 at equivalent design speed and work. Radial surveys at two circumferential positions were made behind each rotor and averaged for a single radial trace. Radial surveys at only one circumferential position (midway between stator blades) were made behind each stator and at only one circumferential position at station 1. The temperature distributions behind the two rotors were obtained with the spike-type total-temperature rakes shown in figure 3(a). Radial surveys of static pressure were not made, because a suitable device for measuring static pressure was not available at the time of the survey. However, the static pressures at the hub and tip behind each blade row and ahead of the first stator were obtained by means of the wall static taps previously described. In correcting the total-temperature and -pressure readings for Mach number effects, a linear variation of static pressure between the measured hub and tip values was assumed.

RESULTS AND DISCUSSION

Over-All Performance

The over-all performance of the turbine is presented in figure 6 as a plot of equivalent work against the flow parameter $\frac{wN}{60\delta}\varepsilon$ for constant values of equivalent speed and rating pressure ratio $p_1'/p_{x,5}'$. In addition, contours of constant brake internal efficiency are shown.

5016

CM-2

At equivalent design work and speed, an efficiency of 0.79 was obtained at a rating pressure ratio of approximately 4.1. The brake internal efficiency at equivalent design work and speed was well below the value anticipated in the design of the turbine. The maximum efficiency obtained was 0.84, occurring at 130 percent of equivalent design speed and a work output of 34.10 Btu per pound, corresponding to a rating pressure ratio of approximately 4.0.

The variation of equivalent weight flow with rating pressure ratio for the equivalent speeds investigated is shown in figure 7. The value for equivalent design weight flow is indicated on the weight-flow ordinate. At equivalent design speed and the rating total-pressure ratio of 4.1 corresponding to equivalent design work, the turbine weight flow was approximately 1 percent greater than the design weight flow. Choking weight flow, indicated when the curves have a zero slope, was obtained above a rating pressure ratio of 2.5 for all speeds. The magnitude of the choking weight flow was the same for all speeds. This indicates that the first stator choked before any other blade row over the range of speeds investigated and controlled the weight flow passed by the turbine.

The variation of equivalent torque with rating pressure ratio for the equivalent speeds investigated is shown in figure 8. Pressure ratios across the turbine great enough to achieve limiting loading were not obtainable. (Limiting loading is defined, for any given speed, as the point at which a further increase in pressure ratio does not produce an increase in torque.)

Axial Static-Pressure Distribution

The static-pressure distribution at the hub of the blades for design speed and various over-all rating pressure ratios $p_1'/p_{x,5}'$ is shown in figure 9. The static pressure at each station is divided by the inlet total pressure in order to minimize the effect of the small fluctuations in inlet total pressure encountered while testing the turbine. The data points are connected by segments of straight lines to help define the individual over-all total-pressure ratios. The design static-pressure distribution through the turbine is also shown in figure 9, by a dashed line.

In addition to comparing the design static-pressure distribution with those actually obtained, figure 9 is useful in determining the choking characteristics of the turbine. Choking in a blade row is indicated when the static pressure at the entrance to the blade row remains constant while the static pressure at the exit of the same blade row decreases as the over-all total-pressure ratio is increased. Based on this criterion, the data indicate that the blade rows choke successively, starting with the first stator, as the over-all total-pressure ratio increases. As mentioned previously, the data plotted in figure 7 indicate that the first stator choked before any other blade row over the range of speeds investigated and controlled the weight flow passed by the turbine.

The maximum over-all pressure ratio shown is less than that required for design work output. However, the static-pressure distribution through the turbine, with the exception of station 5, would not change with increased over-all pressure ratio beyond about 3.8, because all blade rows have choked. The only effect on the static-pressure distribution due to increasing the over-all pressure ratio beyond 3.8 would be to lower the static pressure at station 5. For over-all pressure ratios above 3.8, the static pressure at station 2 is lower than design while at station 3 it is higher than design. This indicates that the effective throat area of the first rotor was too large, resulting in higher than design Mach numbers at the rotor inlet and lower than design at the outlet. It is also quite obvious that the reaction or static-pressure drop across the first rotor was considerably less than design. The static pressure at station 4 was very near the design value. At the exit of the turbine, station 5, the static pressure had to be lowered well below the design value when design work was obtained from the turbine. This, of course, resulted in large tangential components of absolute velocity, which, in turn, were detrimental to the turbine efficiency based on $p'_{x,5}$.

Design-Point Survey

The results of the survey at equivalent design work and speed are presented in figure 10. The absolute-flow-angle distribution behind the first stator (station 2, fig. 10(a)) agreed well with the design distribution. However, the flow was underturned by about 3° over most of the passage height. This difference is not too significant, however, when the mechanical character of the equipment and method of survey are considered. The hub and tip static pressures at station 2 were lower than design, indicating that the absolute Mach numbers were higher than design. These Mach numbers were estimated to be about 0.2 higher than the design values.

The static pressures behind the first rotor (station 3) were higher than design (fig. 9), indicating that the Mach numbers at this station

were lower than design. This was substantiated by the marked underturning of the flow angle from design observed at this station (fig. 10(a)). This underturning became quite extreme near the tip of the blade, indicating a separated-flow region.

The design temperature drop across the first stage was constant over the blade height. As a result of the separation at the tip of the first rotor, however, the temperature drop across the first stage (fig. 10(b)) decreased from midpassage to the tip. This separated region also resulted in a region of low stage efficiency (fig. 10(c)) near the tips of the blades.

The Mach numbers and flow angles obtained at stations 2 and 3 indicate that the effective throat area of the first rotor was too large. The source of the poor performance observed at the tip of the first rotor is more difficult to isolate, however, with the limited survey data available. A detailed investigation of the loss regions in a one-stage turbine (ref. 8) indicated that a major part of the total loss occurred in the tip region of the rotor and that the largest portion of this loss could be attributed to secondary-flow effects. In the investigation of reference 8 another high-loss region of secondary importance was noted near the hub of the rotor. A similar region was observed (see fig. 10(c)) for the first stage of the turbine investigated herein. The loss distribution or efficiency distribution of the first stage investigated herein is similar to that of the single-stage turbine investigated in reference 8; and, therefore, it might be inferred that the sources and proportions of the loss are similar. However, the losses in the rotor tip region of the turbine investigated herein were undoubtedly compounded by the critical design conditions and by the large tip clearances (0.100 in.).

Figure 10(c) shows that the level of the second-stage efficiency was, in general, lower than that of the first stage. This was attributed in part to the large differences between the actual and design flow conditions at the entrance to the second stage (station 3).

The flow at the outlet of the second stator (station 4, fig. 10(a)) was underturned from design by approximately 10° over most of the blade height. However, at the outlet of the second rotor (station 5, fig. 10(a)) the flow was considerably overturned from design. At design work the Mach number at the outlet of the second rotor was higher than design because, with the over-all turbine efficiency considerably less than design, the outlet tangential component of velocity must be increased greatly. This, of course, accounts for the increased negative angles of flow noted at the turbine outlet. The energy of this tangential velocity was considered lost in rating the performance of the turbine (fig. 6). At design work and speed this tangential component of velocity reduced the efficiency by approximately 2.5 percent.

CM-2 back

Both the work output (temperature drop, fig. 10(b)) and the efficiency (fig. 10(c)) fell off at the hub and tip for the second stage of the turbine. The over-all temperature drop and efficiency shown in figures 10(b) and (c) had characteristics similar to those of the first stage. This was to be expected, because 63 percent of the over-all work was achieved by the first stage. The first stage was designed to do 70 percent of the over-all work.

Remarks

The surveys indicate that design flow conditions were not achieved within the turbine, which probably accounts in part for the poor performance. This performance could probably be improved by modifying the turbine. One needed modification is to close down or reduce the throat area of the first-stage rotor, which would reduce the rotor-inlet Mach number and increase the rotor-outlet Mach number. The relative inlet Mach number is quite high, particularly for the type of profile employed; and a reduction of this Mach number should reduce the entering loss. In addition, the angle of incidence on the first-stage rotor would be reduced. With an increased outlet Mach number the absolute flow angle at the outlet of the stage would more nearly approach the design value and, thereby, improve the flow conditions into the second stator. Decreasing the first-stage-rotor throat area would also increase the reaction or static-pressure drop across the blade row and, thus, possibly eliminate or alleviate the separation at the tip of the blade. Shrouding of both rotor blade rows might also help to reduce the losses, since the tip clearances employed (0.100 in.) were quite high.

Another rather serious departure from design flow appeared in the underturning of the flow at the outlet of the second stator. If the total-pressure loss from the turbine inlet to the throat of the second stator is reduced by the modifications just discussed, it would be possible to reduce the second-stator throat area and, thereby, obtain more turning at and after the throat section. An increase of the tangential velocity into the second rotor along with an improvement in over-all turbine efficiency would, of course, mean that design work would not have to be attained by increasing the tangential component of velocity at the outlet of the turbine with its attendant loss. An improvement of the turbine efficiency would also probably require that the throat area of the second rotor be closed down.

In conclusion, it is felt that attainment of reasonably good turbine efficiency is possible with the severe design conditions investigated. However, in designing a turbine of such a critical nature, more refined design techniques that describe actual flow conditions and loss distributions more closely are necessary if good performance is to be obtained without the necessity of an extensive development process. Several of the more advanced techniques being used are presented in references 9 and 10.

SUMMARY OF RESULTS

From an experimental investigation of a high-work-output, low-blade-speed, two-stage turbine operated over a range of equivalent speed and total-pressure ratio at inlet conditions of 35 inches of mercury absolute and 700° R, the following results were obtained:

1. At equivalent design speed and work, the turbine passed 1.01 of the equivalent design weight flow. The brake internal efficiency at this point was 0.79 and occurred at a rating pressure ratio of 4.1.

5016

2. A maximum efficiency of 0.84 occurred at 130 percent of equivalent design speed and a work output of 34.10 Btu per pound, corresponding to a rating total-pressure ratio of approximately 4.0.

3. At equivalent design speed the blade rows choked successively starting with the first stator as the over-all total-pressure ratio increased. The first stator choked before any other blade row over the range of speeds investigated and controlled the weight flow passed by the turbine.

4. A radial survey at equivalent design speed and work revealed:

(a) The effective throat area of the first rotor was too large, resulting in higher than design Mach number at the rotor inlet and lower than design Mach number at the rotor outlet.

(b) A large underturning of the flow at the tip of the first rotor indicated a large amount of separation in this area. A similar, although less severe, situation appeared at the outlet of the second rotor.

(c) Considerable underturning (approximately 10°) occurred over most of the blade height at the outlet of the second stator.

(d) Large tangential components of velocity existing at the turbine outlet amounted to approximately 2.5 points in turbine efficiency.

Lewis Flight Propulsion Laboratory
National Advisory Committee for Aeronautics
Cleveland, Ohio, May 8, 1956

APPENDIX - CALCULATED TOTAL PRESSURE

The equation used to calculate the total pressure at the turbine inlet was obtained from the following equations:

Energy:

$$T' = T + \frac{V^2}{2gJc_p} \tag{1}$$

5016

Continuity:

$$w = \rho VA \tag{2}$$

Perfect gas law:

$$p = \rho RT \tag{3}$$

Isentropic relation:

$$\frac{T}{T'} = \left(\frac{p}{p'}\right)^{\frac{\gamma-1}{\gamma}} \tag{4}$$

For uniform axial flow, based on equations (1) to (4), the following equation for total pressure can be obtained:

$$p' = p\left[\frac{1 + \sqrt{1 + \frac{4T'}{2gJc_p}\left(\frac{R}{p}\right)^2\left(\frac{w}{A}\right)^2}}{2}\right]^{\frac{\gamma}{\gamma-1}} \tag{5}$$

Measurements of static pressure and total temperature were made at the turbine inlet. With the orifice-measured weight flow and annular area also known, the inlet total pressure was calculated from equation (5).

REFERENCES

1. English, Robert E., Silvern, David H., and Davison, Elmer H.: Investigation of Turbines Suitable for Use in a Turbojet Engine with High Compressor Pressure Ratio and Low Compressor-Tip Speed. I - Turbine-Design Requirements for Several Engine Operating Conditions. NACA RM E52A16, 1952.

2. Davison, Elmer H., and English, Robert E.: Investigation of Turbines Suitable for Use in a Turbojet Engine with High Compressor Pressure Ratio and Low Compressor-Tip Speed. II - Velocity-Diagram Study of Turbine for Engine Operation with Constant Exhaust-Nozzle Area. NACA RM E52D14, 1952.

3. English, Robert E., and Davison, Elmer H.: Investigation of Turbines Suitable for Use in a Turbojet Engine with High Compressor Pressure Ratio and Low Compressor-Tip Speed. III - Velocity-Diagram Study of Two-Stage and Downstream-Stator Turbines for Engine Operation at Constant Rotative Speed. NACA RM E52G15, 1952.

4. Davison, Elmer H., and English, Robert E.: Investigation of Turbines Suitable for Use in a Turbojet Engine with High Compressor Pressure Ratio and Low Compressor-Tip Speed. IV - Effect of Increasing Blade Speed on Velocity Diagrams of Turbine for Engine Operation at Constant Rotative Speed. NACA RM E52H13, 1952.

5. Davison, Elmer H., Petrash, Donald A., and Schum, Harold J.: Investigation of Turbines Suitable for Use in a Turbojet Engine with High Compressor Pressure Ratio and Low Compressor-Tip Speed. V - Experimental Performance of Two-Stage Turbine with Downstream Stator. NACA RM E55H16, 1955.

6. Huppert, M. C., and MacGregor, Charles: Comparison Between Predicted and Observed Performance of Gas-Turbine Stator Blade Designed for Free-Vortex Flow. NACA TN 1810, 1949.

7. Rebeske, John J., Jr., Berkey, William E., and Forrette, Robert E.: Over-All Performance of J35-A-23 Two-Stage Turbine. NACA RM E51E22, 1951.

8. Whitney, Rose L., Heller, Jack A., and Hauser, Cavour H.: Investigation of Distribution of Losses in a Conservatively Designed Turbine. NACA RM E53A16, 1953.

9. Stewart, Warner L., Wong, Robert Y., and Evans, David G.: Design and Experimental Investigation of Transonic Turbine with Slight Negative Reaction Across Rotor Hub. NACA RM E53L29a, 1954.

10. Miser, James W., Stewart, Warner L., and Monroe, Daniel E.: Effect of High Rotor Pressure-Surface Diffusion on Performance of a Transonic Turbine. NACA RM E55H29a, 1955.

5016

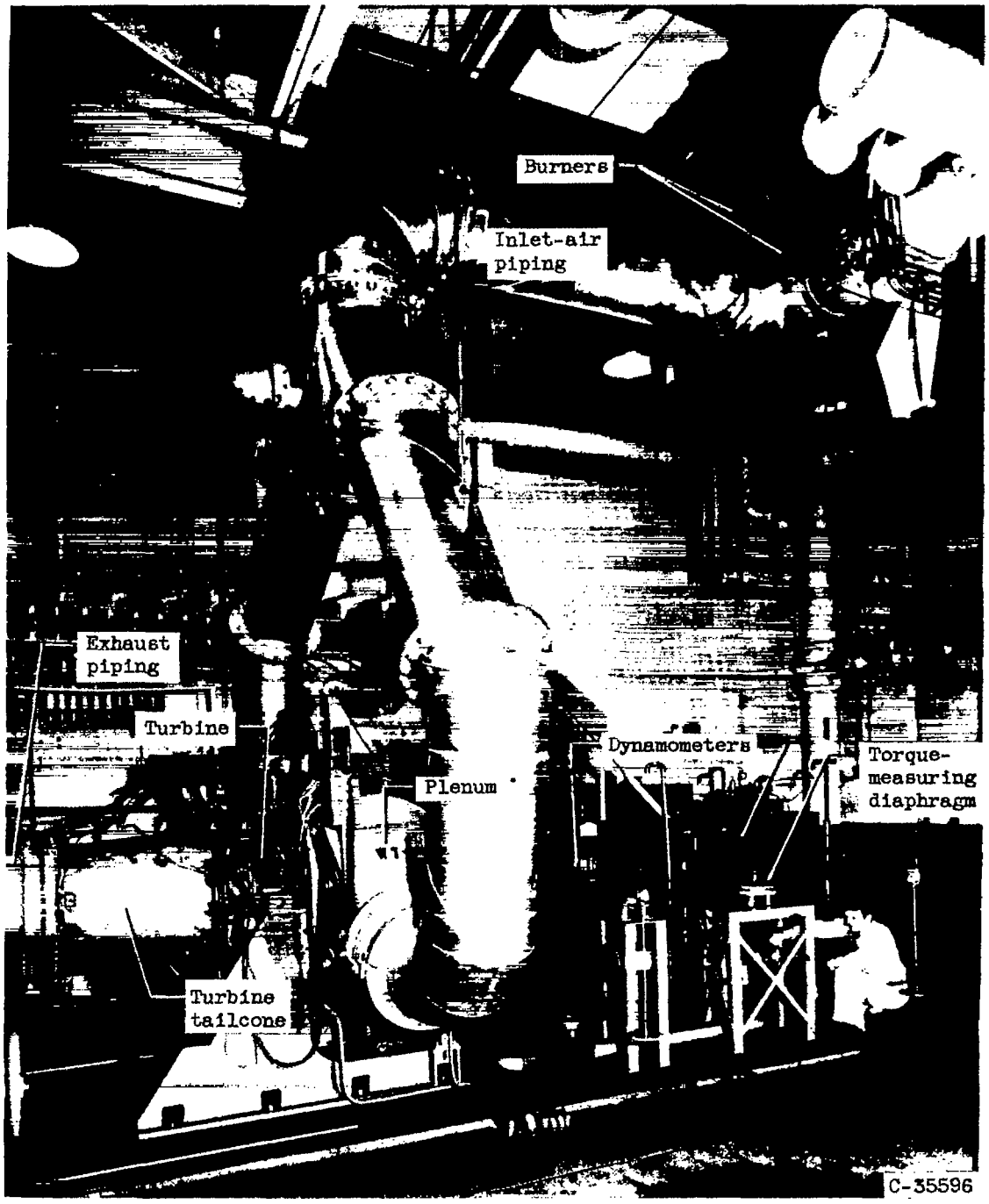

Figure 1. - Installation of turbine in full-scale turbine-component test facility.

5016

CM-3

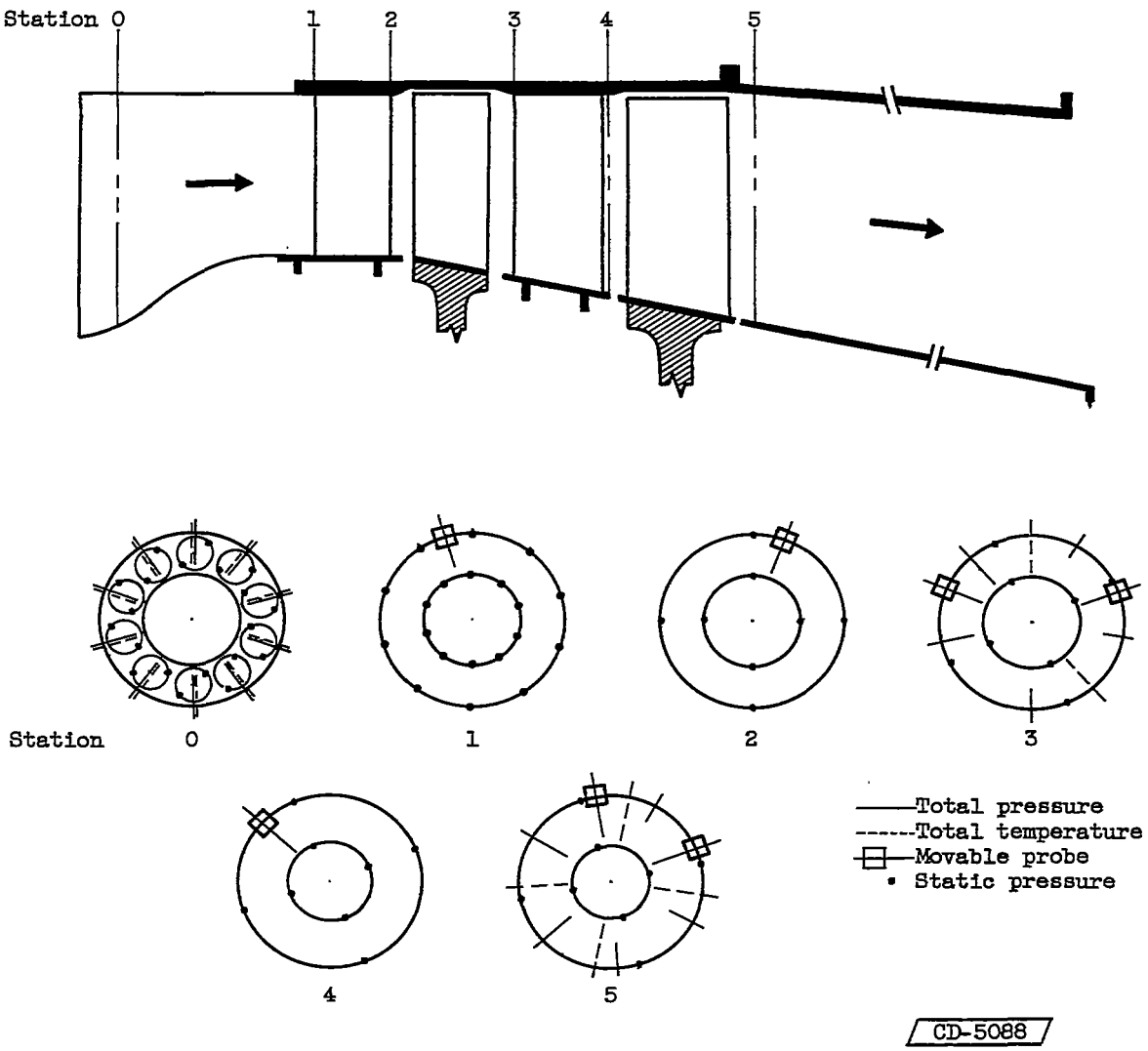

Figure 2. - Schematic diagram of turbine showing instrumentation.

5016

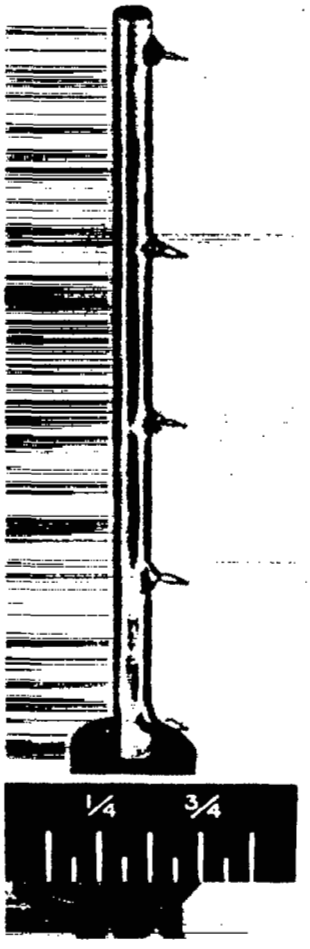

(a) Total-temperature rake.

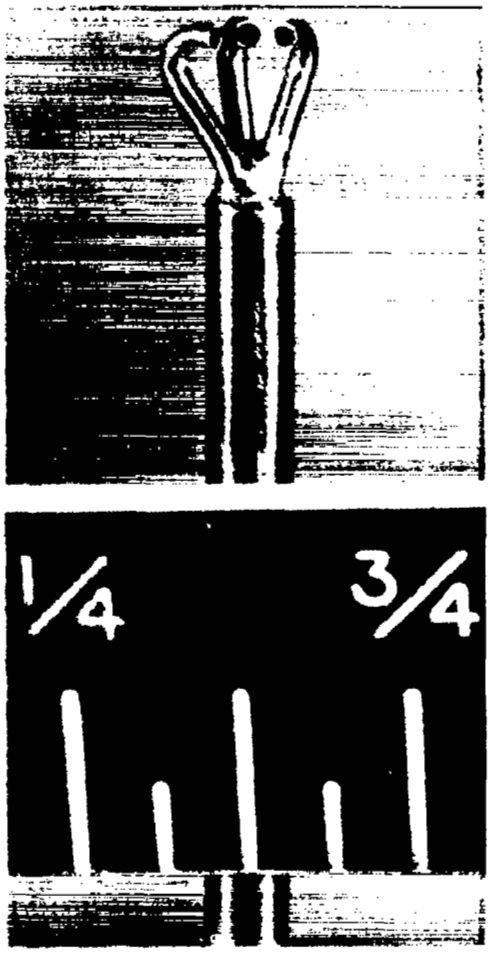

(b) Claw-type survey probe, total pressure and angle.

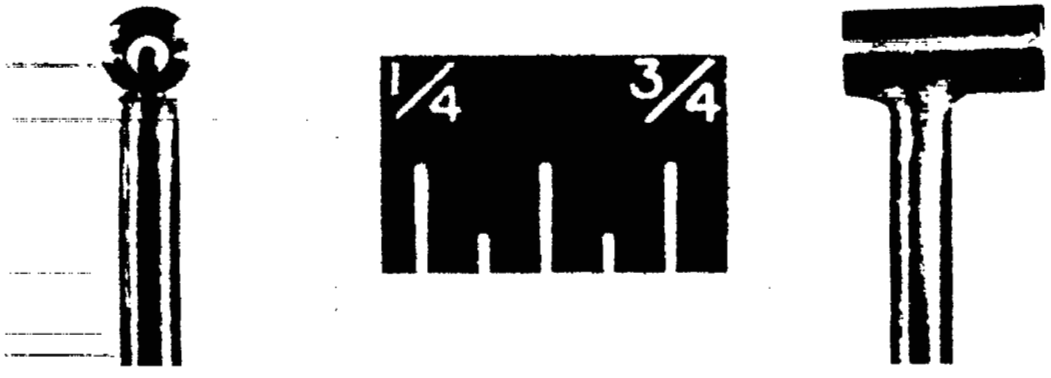

C-41981

(c) Total-pressure probe.

Figure 3. - Typical instruments.

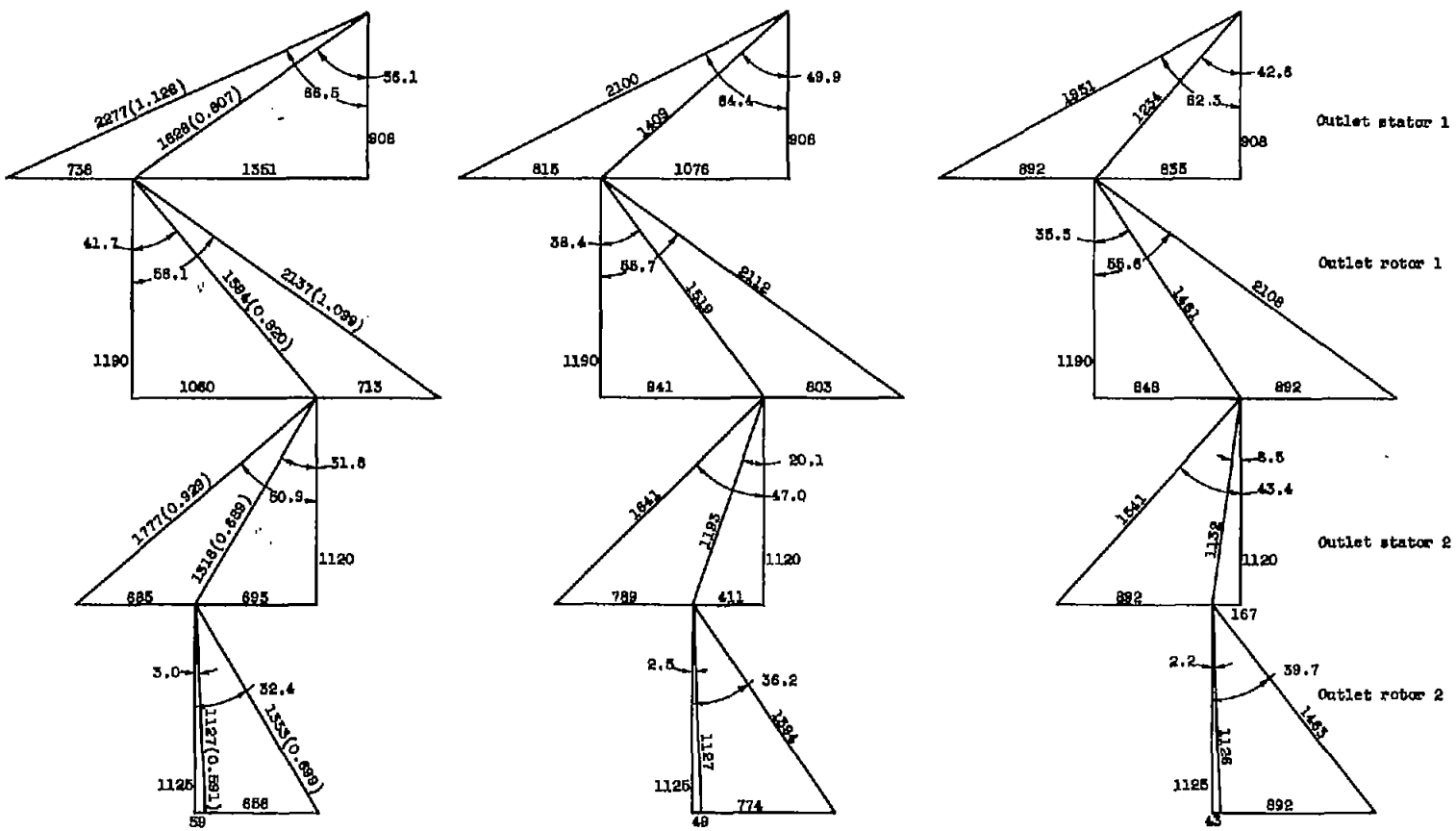

(a) Hub. (b) Mean. (c) Tip.

Figure 4. - Design velocity diagrams. Numbers in parentheses are Mach numbers based on local velocity of sound; velocities are in feet per second; angles are in degrees (ref. 2).

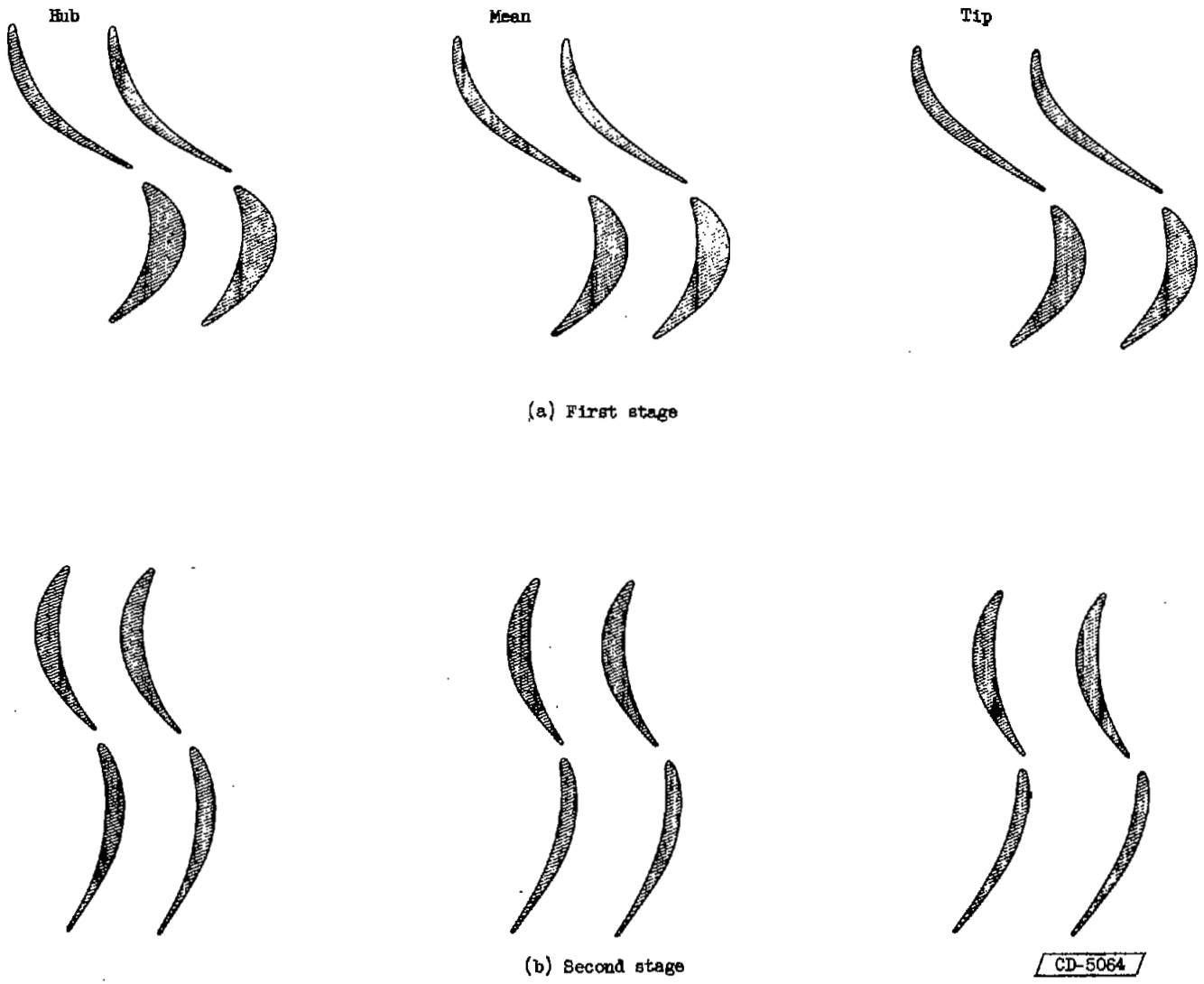

(a) First stage

(b) Second stage

Figure 5. - Design blade and channel shapes for two-stage turbine.

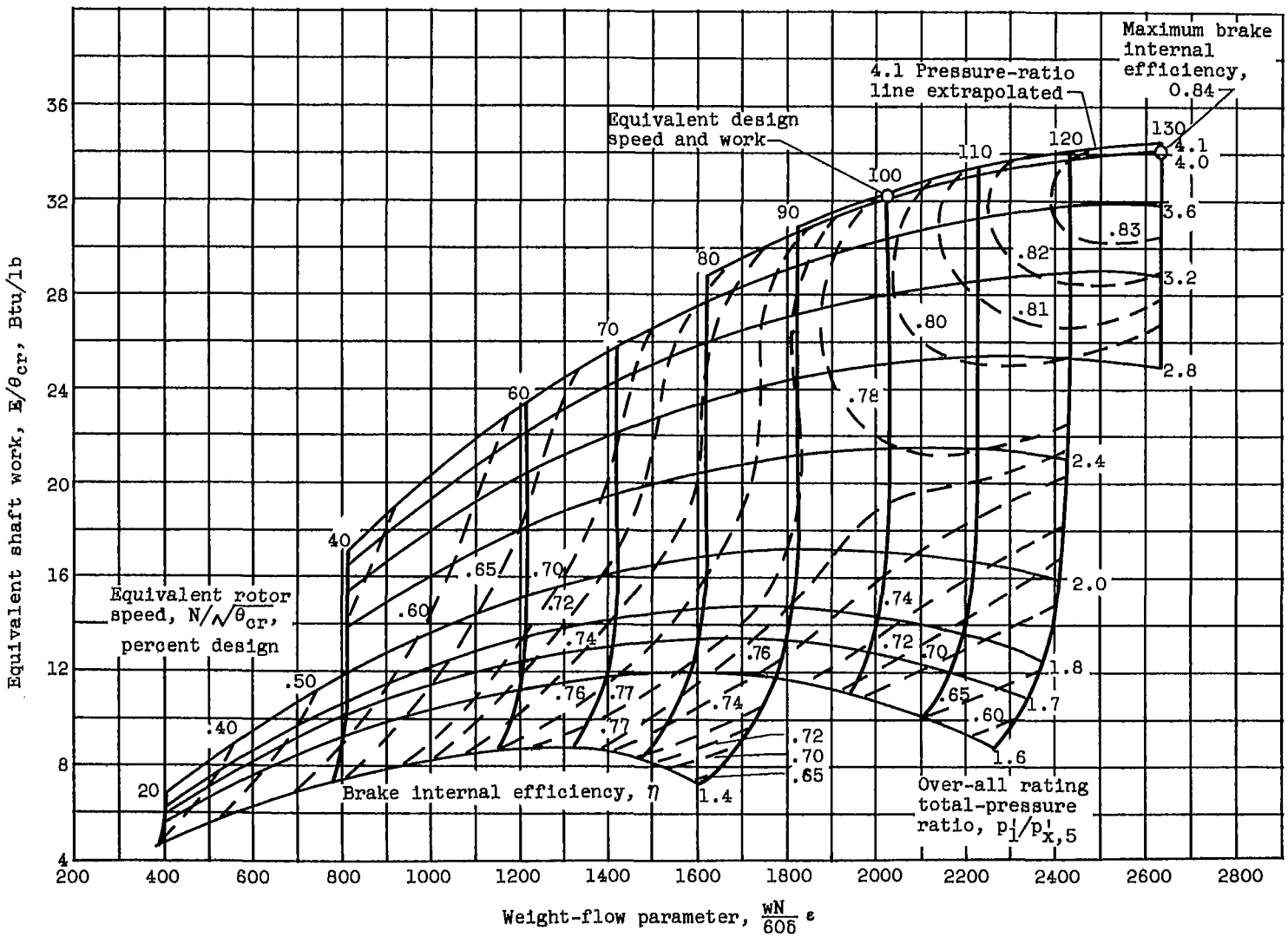

Figure 6. - Over-all performance of turbine. Turbine-inlet pressure, 35 inches of mercury absolute; turbine-inlet temperature, 700° R; equivalent design speed, 3027 rpm.

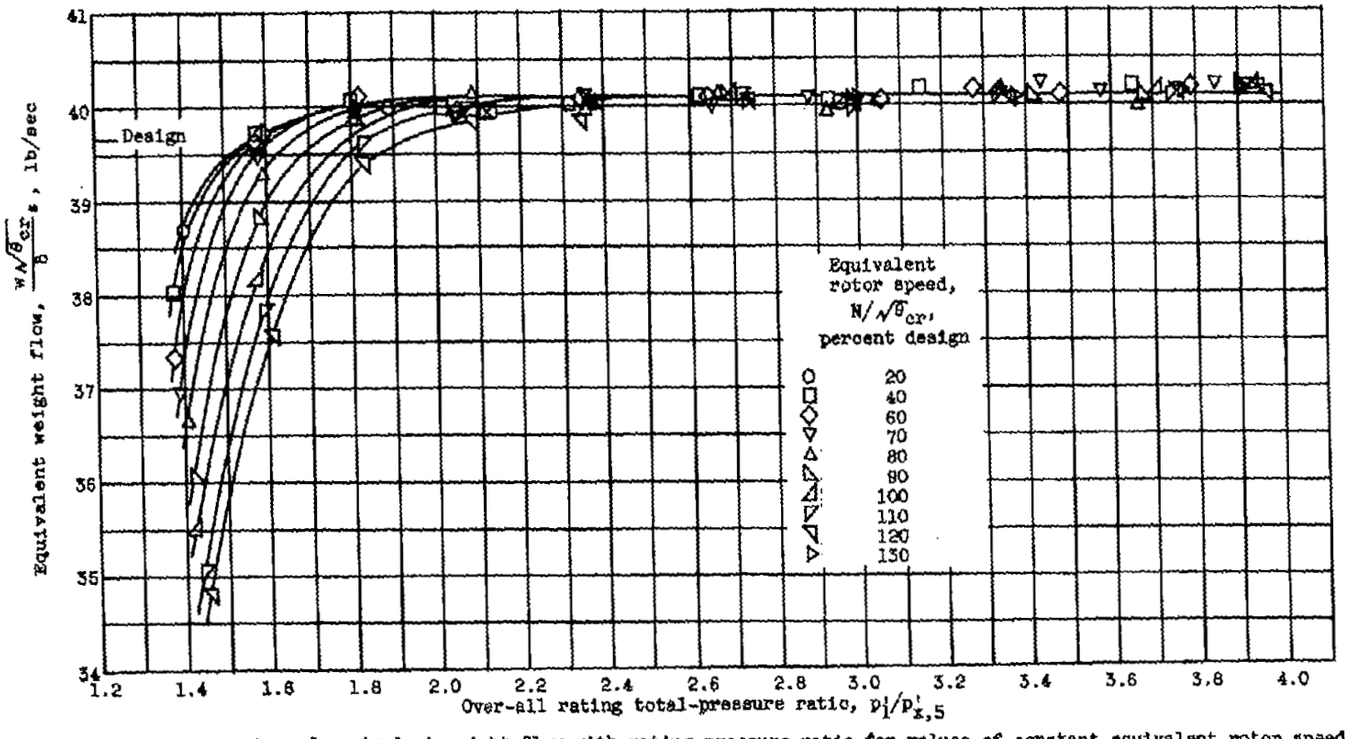

Figure 7. - Variation of equivalent weight flow with rating pressure ratio for values of constant equivalent rotor speed.

5016

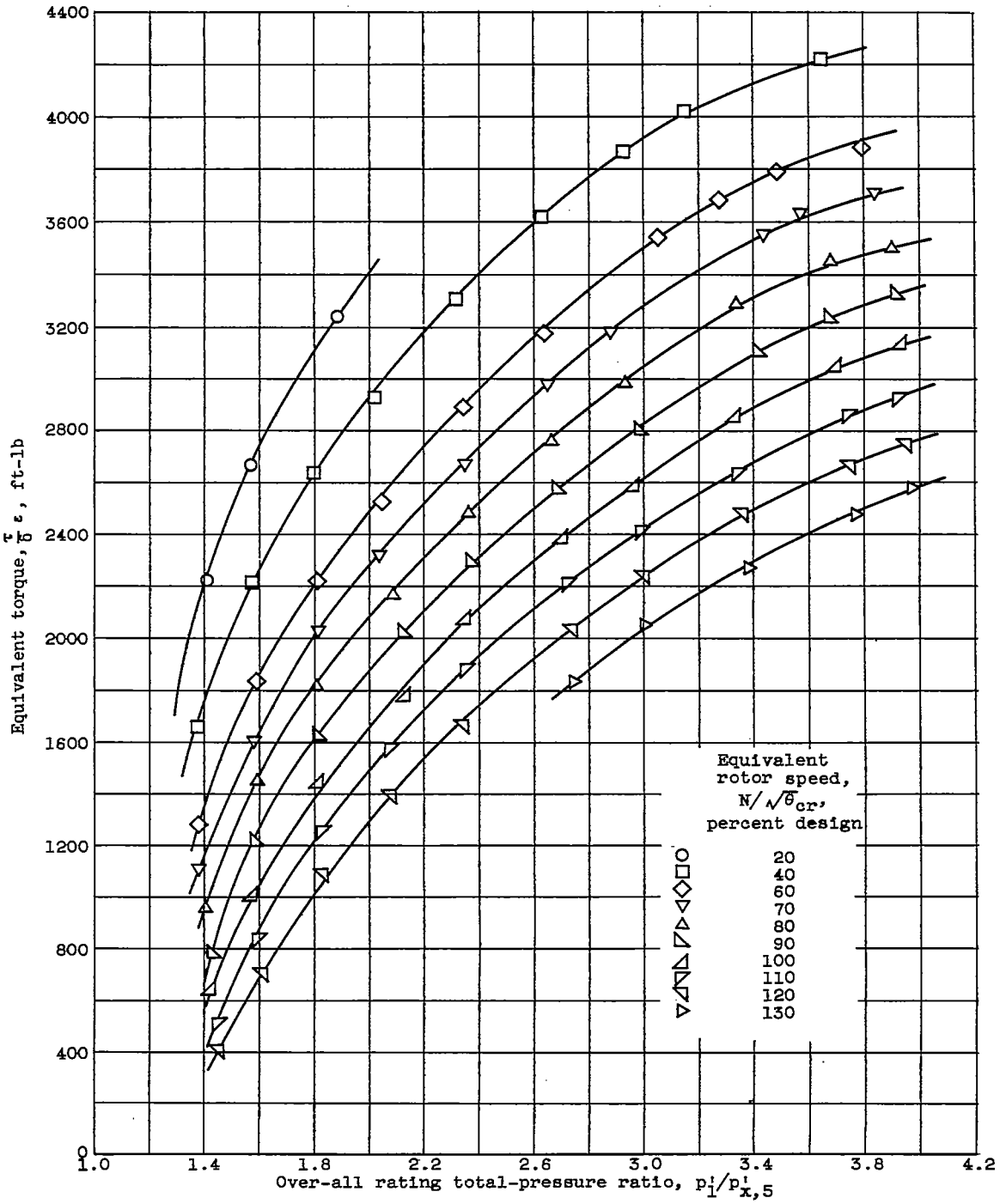

Figure 8. - Variation of equivalent torque with rating total-pressure ratio for values of constant equivalent rotor speed.

5016

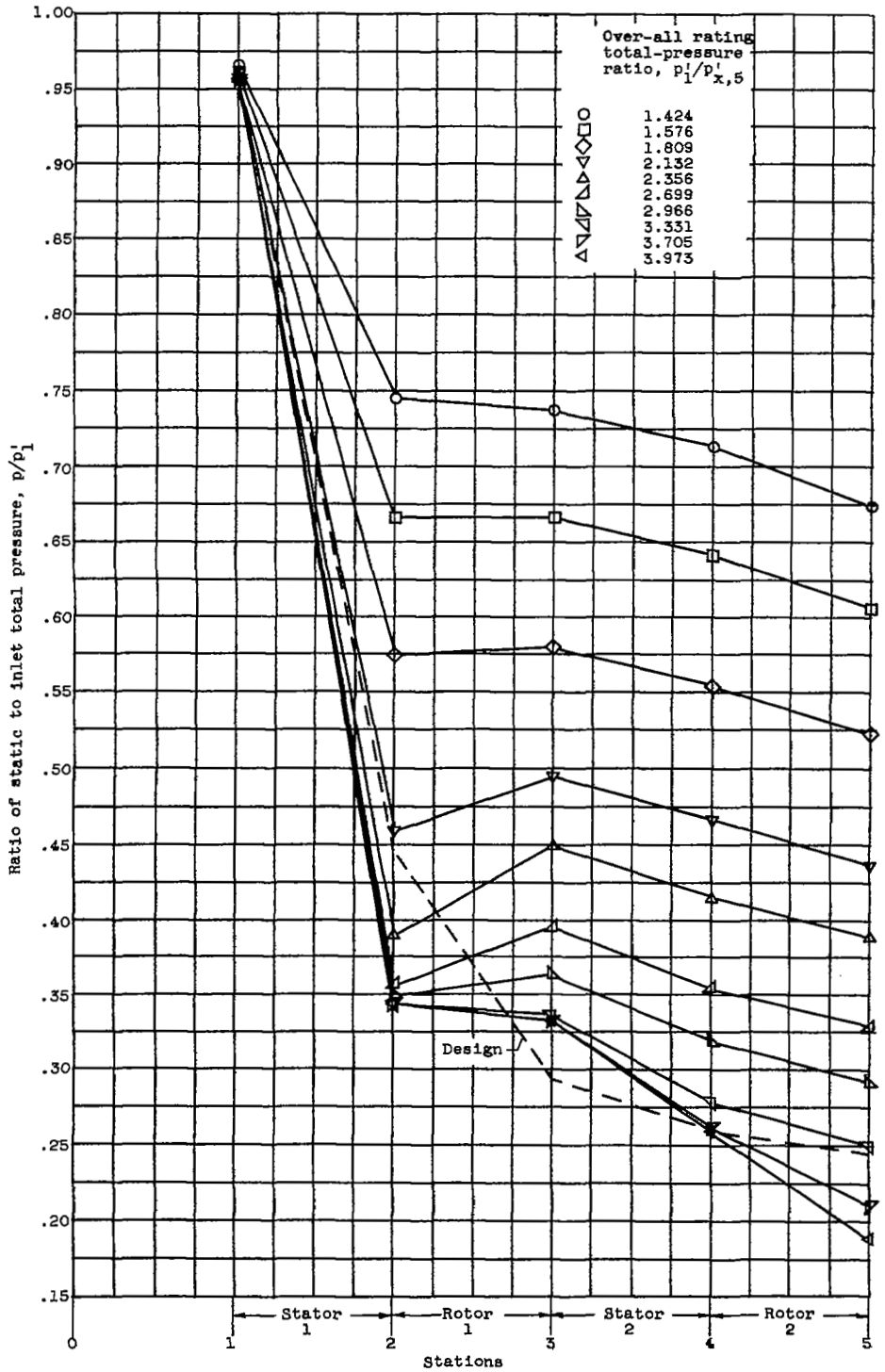

Figure 9. - Variation of hub static-pressure distribution with rating total-pressure ratio at equivalent design speed.

[redacted]

[redacted]

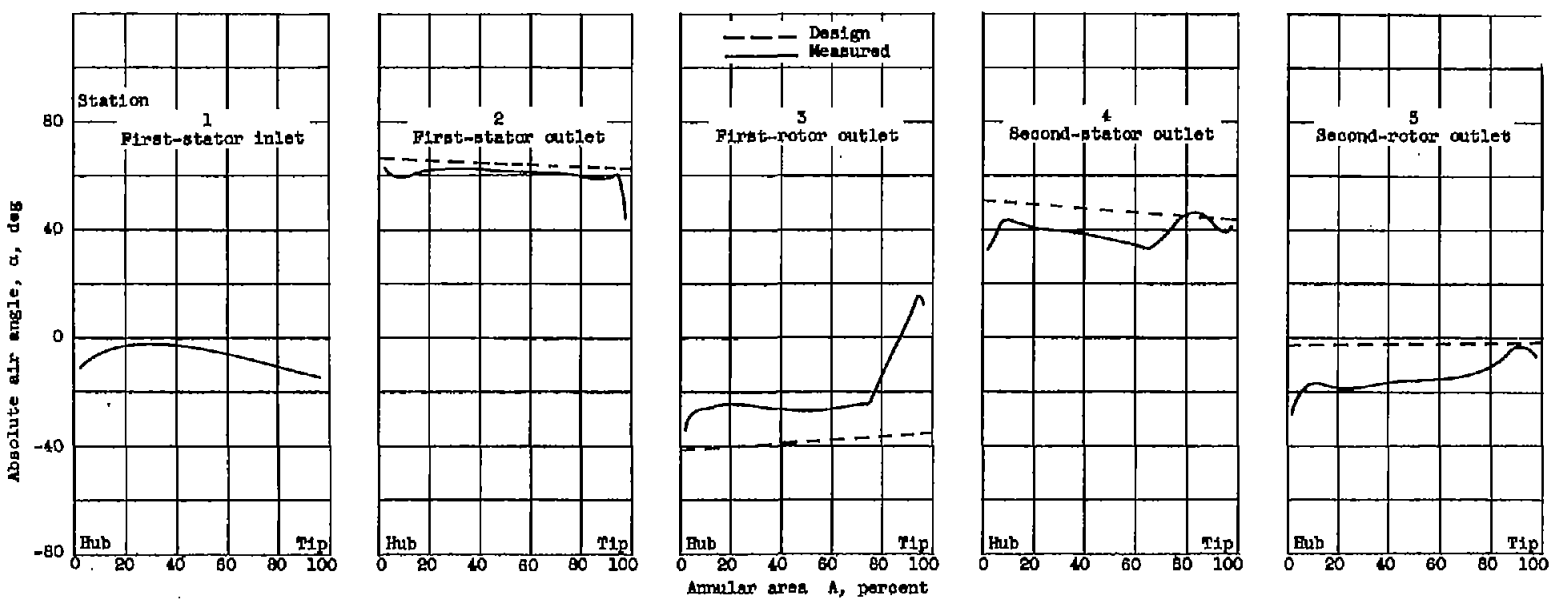

(a) Absolute air angle, measured from axial.

Figure 10. - Radial variation of absolute air angle, work parameter, and efficiency at design speed and work.

[redacted]

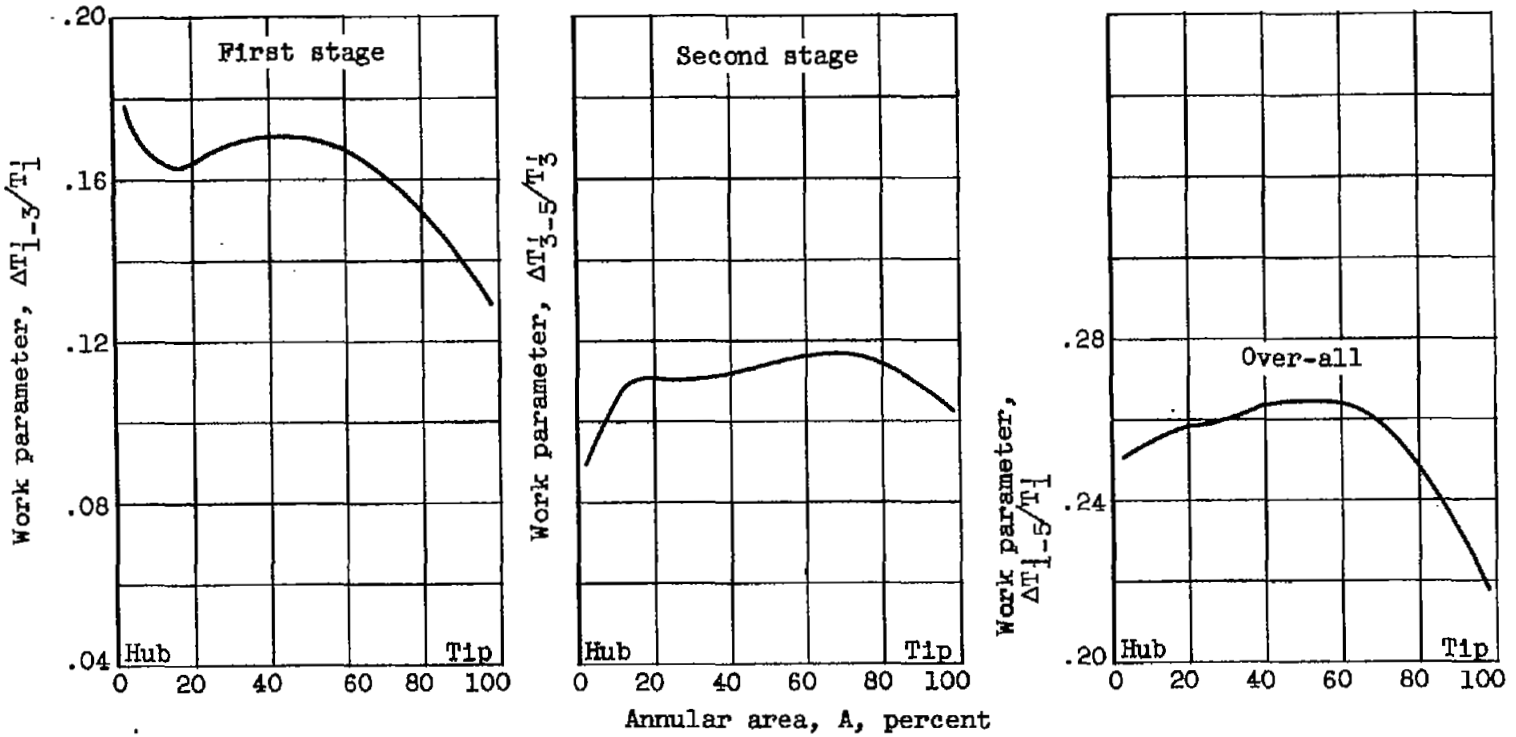

(b) Stage and over-all work parameter.

Figure 10. - Continued. Radial variation of absolute air angle, work parameter, and efficiency at design speed and work.

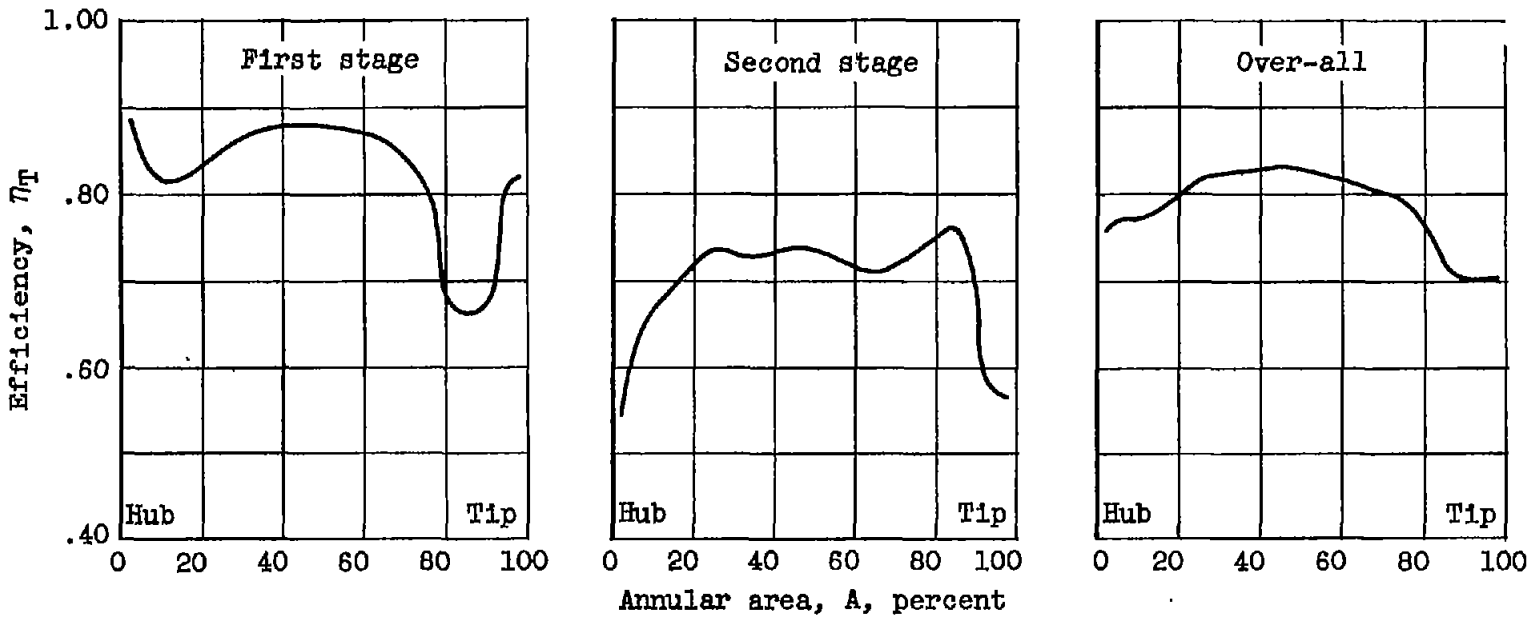

(c) Stage and over-all internal efficiency.

Figure 10. - Concluded. Radial variation of absolute air angle, work parameter, and efficiency at design speed and work.

NACA - Langley Field, Va.

[redacted]

NASA Technical Library
3 1176 01435 8510

[redacted]